Photoaged Skin Therapy with Adipose-Derived Stem Cells

Luiz Charles-de-Sá, M.D., Ph.D.
Natale Ferreira Gontijo-de-Amorim, M.D., Ph.D.
Gino Rigotti, M.D., Ph.D.
Andrea Sbarbati, M.D., Ph.D.
Paolo Bernardi, Ph.D.
Donatella Benati, Ph.D.
Rosana Bizon Vieira Carias, Ph.D.
Christina Maeda Takiya, M.D., Ph.D.
Radovan Borojevic, Ph.D.

Rio de Janeiro, Brazil; and Verona, Italy

Background: The major intrinsic cause of facial skin degeneration is age, associated with extrinsic factors such as exposure to sun. Its major pathologic causes are degeneration of the elastin matrix, with loss of oxytalan and elaunin fibers in the subepidermal region, and actinic degeneration of elastin fibers that lose their functional properties in the deep dermis. Therapy using autologous adipose mesenchymal stem cells for regeneration of extracellular matrix in patients with solar elastosis was addressed in qualitative and quantitative analyses of the dermal elastic fiber system and the associated cells.

Methods: Mesenchymal stem cells were obtained from lipoaspirates, expanded in vitro, and introduced into the facial skin of patients submitted after 3 to 4 months to a face-lift operation. In the retrieved skin, immunocytochemical analyses quantified elastic matrix components; cathepsin K; matrix metalloproteinase 12 (macrophage metalloelastase); and the macrophage M2 markers CD68, CD206, and hemeoxygenase-1.

Results: A full de novo formation of oxytalan and elaunin fibers was observed in the subepidermal region, with reconstitution of the papillary structure of the dermal-epidermal junction. Elastotic deposits in the deep dermis were substituted by a normal elastin fiber network. The coordinated removal of the pathologic deposits and their substitution by the normal ones was concomitant with activation of cathepsin K and matrix metalloproteinase 12, and with expansion of the M2 macrophage infiltration.

Conclusion: The full regeneration of solar elastosis was obtained by injection of in vitro expanded autologous adipose mesenchymal stem cells, which are appropriate, competent, and sufficient to elicit the full structural regeneration of the sun-aged skin. (*Plast. Reconstr. Surg.* 145: 1037e, 2020.)

CLINICAL QUESTION/LEVEL OF EVIDENCE: Therapeutic, IV.

Stem cell therapy for repair and regeneration of tissues and organs damaged by trauma or degeneration is now used in many fields of medicine. The mesenchymal stem cells are one of the major stem cell types used in regenerative medicine. They can be obtained from several tissues, including the subcutaneous adipose tissue, and used either immediately or after their expansion in vitro.[1] The latter approach may be

From the Programa de Pós-Graduação em Ciências Cirúrgicas and the Instituto de Biofísica Carlos Chagas Filho, Laboratório de Imunopatologia, Universidade Federal do Rio de Janeiro; the Dipartamento di Scienze Neurologiche e del Movimento, Sezione di Anatomia e Istologia della Universitá degli Studi di Verona; the Unità di Chirurgia Rigenerativa dela Clinica San Francesco; and the Centro de Medicina Regenerativa, Faculdade de Medicina de Petrópolis.
Received for publication April 4, 2018; accepted March 27, 2019.
The first three authors contributed equally to this article.
This trial is registered under the name "Cutaneous Analysis after Adipose Mesenchymal Cells from Stromal Vascular Fraction Applied in Human Face," Brazilian Clinical Trials Registry no. RBR-2nn9y2 (http://www.ensaiosclinicos.gov.br/rg/RBR-2nn9y2/).

DOI: 10.1097/PRS.0000000000006867

Disclosure: *The authors have no competing interests to disclose.*

Related digital media are available in the full-text version of the article on www.PRSJournal.com.

A "Hot Topic Video" by Editor-in-Chief Rod J. Rohrich, M.D., accompanies this article. Go to PRSJournal.com and click on "Plastic Surgery Hot Topics" in the "Digital Media" tab to watch.

preferable to reach the required cell quantity, or potentially cryopreserve cells for future use, and this was done in the present study.

Mesenchymal stem cells have been used extensively in skin therapies, because they have a broad paracrine action on dermal cells; they stimulate angiogenesis; they protect other cells from the peroxide-mediated damage; and also modulate inflammation, pain, and immune tolerance.[2–4] The use of adipose-derived stem cells in skin has been described in diverse clinical studies, with satisfactory results.[5–8] Experimental studies suggested also the role of adipose-derived stem cells in improving quality of the aging skin, but we still need extensive clinical studies concerning the histologic changes of the human skin that was exposed to local interaction with adipose-derived stem cells. The structural changes that occur in the skin, which can justify the observed long-lasting improvement that is visible and reported after fat grafts, are still not well known.

In the skin showing photoaging, a progressive degeneration of the entire elastin network occurs in the deep dermis. Major elastic fibers become thickened, tangled, tortuous, degraded, and dysfunctional, setting the solar actinic elastosis, the most relevant feature of the photoaged skin. The overall marked loss of collagen and the thickening of elastic fibers cause accumulation of the dysfunctional elastic component in the skin of elderly humans compared with young ones.[9,10] The purpose of the present study was to investigate the effects of adipose-derived stem cell therapeutic introduction into the facial skin of patients with overt photoaging, with special attention to morphologic modifications of the dermal extracellular matrix.

PATIENTS AND METHODS

Surgical Technique

This clinical, prospective study involved 20 healthy subjects, 16 women and four men, aged 45 to 65 years, candidates for facial rejuvenation surgery (face lifting). They were inhabitants of the northeast region of Brazil, where extensive exposure to sun is expected, and they presented Fitzpatrick class IV (n = 9) and class V (n = 11) skin types.[11] The study was conducted between September of 2012 and June of 2014. Patients were treated according to the ethical principles of the Declaration of Helsinki 2000, and the present study was approved by the Brazilian Medical Investigation Ethical Board (protocol no. 28063) and deposited in the Brazilian Clinical Trials Registry (RBR-2nn9y2).

All of the patients received extensive information on the protocols and outcomes. They signed informed consent documents to participate in the study and to leave available materials and data for the analyses of results. Subjects who smoked; those with hematologic or hemodynamic disorders, autoimmune diseases, connective tissue diseases, diabetes type 1 or 2, other metabolic diseases, or chronic use of corticosteroids; and those that had been submitted to recent dermatologic (minimum, 6 months without skin treatment) or surgical treatments (e.g., facial peeling) were excluded. The direct endpoint of the study was to assess the histologic benefits provided by the subdermal adipose-derived stem cell injection. The introduction of in vitro expanded autologous adipose tissue–derived mesenchymal stem cells was followed by the clinical monitoring of potential adverse effects for 3 to 4 months.

Adipose-derived Stem Cell Harvesting, Isolation, and Expansion

Under local anesthesia with 0.5% lidocaine and 1.5 million U epinephrine, 10 cc of adipose tissue from the infraabdominal region was manually harvested by liposuction, using a 10-ml syringe (Luer-Lok; Becton, Dickinson & Co., Franklin Lakes, N.J.) coupled to a liposuction cannula 3 mm in diameter and 15 cm long, containing three distal holes (Tulip Medical Products, San Diego, Calif.). A light negative pressure was created by slowly withdrawing the syringe plunger by hand to harvest fat tissue. The lipoaspirate was transferred to a glass vial containing Roswell Park Memorial Institute medium and antibiotics (amphotericin and ciprofloxacin) and transported in a temperature-controlled container (4°C) to the laboratory to isolate and expand adipose-derived stem cells within 24 hours.

Following the standard protocols,[12] a 10-ml sample of the lipoaspirate was dissociated with collagenase IA (Sigma-Aldrich, St. Louis, Mo.), 200 U/mg of tissue, and incubated at 37°C under constant agitation for 1 hour. The material was then centrifuged, and the pellet was filtered through a nylon mesh of 70 μm. The cells were resuspended in culture medium supplemented with 10% fetal bovine serum, quantified using trypan blue, and plated in low-glucose Dulbecco's Modified Eagle Medium supplemented with 20% fetal bovine serum and antibiotics (100 U/ml penicillin and 100 μg/ml streptomycin). Cultures were maintained at 37°C under 5% carbon

dioxide. The following day, nonadherent cells were removed, and adherent cells were expanded by replating when reaching early confluence as described previously.[13,14] Their differentiation capacity was confirmed under appropriate induction, and phenotype was characterized by cytometry, as described previously.[14] This whole process lasted 3 weeks. Two days before application, the cells were washed with physiologic saline and incubated in the culture medium supplemented with autologous plasma at 37°C under 5% carbon dioxide. One day before application, 1-ml Luer-Lok–type syringes, containing 2 million cells in 0.4 ml phosphate-buffered solution, were prepared and transported to the ambulatory facilities for subdermal injection, in an area of 1 cm^2 skin surface of the preauricular region, 2 cm distally from the tragus.

Skin Biopsy Specimens

The nontreated skin biopsy specimens (0.5 × 1 cm) were excised under local anesthesia with lidocaine 0.5% and epinephrine 1.5 million U in the preauricular area, 0.5 cm away from the tragus. Biopsy specimens of adipose-derived stem cell–treated skin were taken from 1.5 to 2 cm away from the tragus after a 3- to 4-month interval, during face lifting.[15]

Immunohistochemistry

Paraffin sections were obtained and submitted to immunohistochemical techniques. The following antibodies were used: anti-tropoelastin (rabbit polyclonal, PR398; Elastin Products Co., Owensville, Mo.), anti–fibrillin-1 (rabbit polyclonal, PR217; Elastin Products), anti-elastin (rabbit polyclonal, ab21607; Abcam, Cambridge, Mass.), anti–matrix metalloproteinase 12 (rabbit monoclonal; Abcam), anti–cathepsin K (mouse monoclonal, clone EP1261Y, ab52897; Abcam), anti-CD68 (monoclonal mouse, clone KPi; Dako, Carpinteria, Calif.), anti-mannose receptor (rabbit polyclonal, 64693; Abcam), and hemeoxigenase-1 (rabbit polyclonal, ab13243; Abcam).

After dewaxing and hydrating, sections were incubated in a solution of 50 mM ammonium chloride in phosphate-buffered saline (pH 8.0) for 30 minutes, permeabilized with 0.5% triton X-100 in phosphate-buffered saline, followed by inhibition of endogenous peroxidase with 3% hydrogen peroxide in methanol, and submitted to heat-mediated antigen retrieval. After blocking the nonspecific binding of immunoglobulins with 5% bovine serum albumin, sections were incubated with the specific antibodies for 16 hours in a humid chamber at 4°C. After washing with phosphate-buffered saline 0.25% Tween-20 solution, primary antibodies were revealed with either the EnVision-horseradish peroxidase kit (Dako) or with CSA-II, biotin-free catalyzed amplification system horseradish peroxidase (catalogue no. K-1497; Dako) for cathepsin K and matrix metalloproteinase 12. The chromogen used for peroxidase visualization was diaminobenzidine (Liquid DAB; Dako). All reactions were performed using positive controls (breast cancer for matrix metalloproteinase 12, and kidney biopsy sections for cathepsin K) and negative controls (instead of primary antibody, incubation with the same immunoglobulin isotype).

Histomorphometry

High-resolution images (2048 × 1536 pixels) were captured with a system of image analysis consisting of a digital photographic machine (Evolution VR Cooled Color 13 bits; Media Cybernetics, Bethesda, Md.) coupled to a light microscope (Eclipse E800; Nikon, Tokyo, Japan). For the capture of images, the software Q-Capture 2.95.0, release 2.0.5 (Silicon Graphics, Inc., Sunnyvale, Calif.) was used. After program settings and calibration of color and contrast for each type of stain, the Image-Pro Plus 4.4.1 software (Media Cybernetics) was used for quantification of either the stained or the immunostained slides.

Statistical Analyses

Data were analyzed using SAS 6.112 (SAS Institute, Inc., Cary, N.C.), and expressed as medians (interquartile range). The Wilcoxon signed rank test was used for data analysis. An overall α level of 0.05 was used as the limit of statistical significance.

RESULTS

Patient Follow-Up

The 20 patients that participated in the present study (16 women and four men) were followed for 3 to 4 months after the subdermal adipose-derived stem cell injection, until the skin removal was performed during face-lift surgery. The patients ranged in age from 45 to 65 years (mean ± SEM, 56 ± 2.53 years), and body mass index ranged from 22 to 30 kg/m^2 (mean ± SEM, 24.4 ± 0.554 kg/m^2). Local transitory effects were occasionally observed immediately after the cell injection, such as injection-site erythema, edema,

bruising, or induration. These effects did not require any clinical treatment, and the patients returned to the normal skin condition within less than 48 hours. No later skin reactions were observed, such as persisting inflammation, necrosis, hyperplasic or abnormal cell growth, tumor development, or any other adverse events such as vasculitis or hypertrophic scars. On clinical analyses, considerable local improvement of the skin quality was observed.

The late follow-up of the subjects that participated in the present study reaches at present more than 1 year. We did not detect any late adverse effects that could be potentially related to the cell injection, similar to the published data on meta-analyses concerning local or systemic injections of adipose-derived stem cells of diverse origins, which involved more than 1000 patients.[16]

Characterization by Flow Cytometry (Fluorescence-Activated Cell Sorting) and In Vitro Differentiation of Adipose-Derived Stem Cells

Adipose-derived stem cells were characterized using combinations of surface markers of the mesenchymal cells, pericytes, and fibroblasts: CD105, CD90, CD73, CD14, CD45, CD34, and HLA-DR. The cells were expanded for four to five passages before application, when they were characterized by flow cytometry using the appropriate monoclonal antibodies. We observed that 88.9 ± 6.5 percent of cells were positive for CD105, CD90, and CD73; and 99.4 ± 0.4 percent were negative for CD14, CD45, CD34, and HLA-DR.

Patient Skin Histopathology before and after Adipose-Derived Stem Cell Treatment

All the subjects included in the present study had solar elastosis consequent to skin photoaging, caused by chronic exposure to sun. The candidates that participated in the study had spontaneously chosen the face-lifting surgical procedure at its end, indicating that they were not satisfied with the overall state of their facial image and skin flaccidity.

The major dermal structure involved in photoaging was the elastin component of the dermal extracellular matrix. The normal presence and orientation of oxytalan, elaunin, and elastic fibers in healthy young skin are depicted. The histologic analysis of skin samples, collected within the studied group before treatment, showed a consistent overall photoaged pathologic condition, albeit it was present at different degrees of intensity. The dermal-epidermal junction was flattened, with a reduction or a full loss of the dermal papillae. The underlying zone 1 of the dermis was identified as the grenz zone,[17] showing an extensive loss of both elaunin and oxytalan fiber networks, without inflammation. Zone 2 was the major site of deposits of degenerated elastic fibers and of the scattered elastotic material derived from damaged fibers, with accumulation of dense clumps of orcein-stained material in the lower limit of papillary dermis and in the reticular dermis. In this zone, hematoxylin and eosin staining showed a variable number of inflammatory cells, basophilic degeneration of connective tissue fibers, and perivascular interstitial edema. [**See Figure, Supplemental Digital Content 1**, which shows the elastic fiber system in human young facial skin (*left*) and in aged sun-exposed skin (*right*). (*Left*) Papillary dermis shows thin oxytalan fibers perpendicular to the dermal-epidermal junction arising from a thicker elaunin fibers plexus. In the underlying reticular dermis, a plexus of elastic fibers of the dermis is mostly parallel to the dermal-epidermal junction (orcein staining with previous oxidation; original magnification, × 40); *scale bar* = 25 μm. (*Right*) Disorganization of the elastic fiber system is shown, with accumulation of elastotic material. Note the absence of oxytalan and elaunin fibers in zone 1 of the dermis. Elastosis is seen in zone 2 (orcein staining with previous oxidation; original magnification, × 40); *scale bar* = 25 μm, ***http://links.lww.com/PRS/E84***.]

Semiquantitative Comparative Analysis of the Selected Histologic Parameters before and after Adipose-Derived Stem Cell Treatment

The parameters selected for this semiquantitative comparative analysis deal with overall modifications of the histopathology observed after treatment. They indicated an increased interaction of the treated photoaged skin with the body fluid flow, and with the associated input of circulating cells. The significantly increased angiogenesis was indeed associated with the equivalent increase of perivascular and interstitial edema. Angiogenesis, inflammation, and basophilic degeneration were quantified following a numeric score ranging from grade 0 to grade 4 (hematoxylin and eosin stain). Differences between both groups were evaluated by the Wilcoxon signed rank test ($p < 0.05$; $n = 20$).

Patient Dermal Elastic Fibers System before and after Adipose-Derived Stem Cell Treatment

All biopsy specimens of facial sun-aged skin submitted to subdermal injection of autologous adipose tissue–derived mesenchymal stem cells showed different degrees of improvement of the overall skin structure, with partial or extensive reversal of the pathologic signs typical of solar elastosis. Histopathologic analyses indicated that the elastin component of extracellular matrix of the skin was apparently the major target of the therapy.

In the dermis zone 1, devoid of the oxytalan and elaunin elastic network in the solar elastosis samples (Fig. 1, *above*, *left*), a fully organized new network was found after the treatment. The regularly spaced oxytalan fiber bundles were crossing the region under the dermal-epidermal junction perpendicularly, linking it to the subjacent diffuse elastin fiber network laid parallel to the skin surface (Fig. 1, *above*, *right*). The quantitative analysis confirmed a significant increase ($p = 0.0001$) of new elastic fibers present in zone 1 with intense neoelastogenesis in the regeneration of the solar elastosis (Fig. 1, *below*).

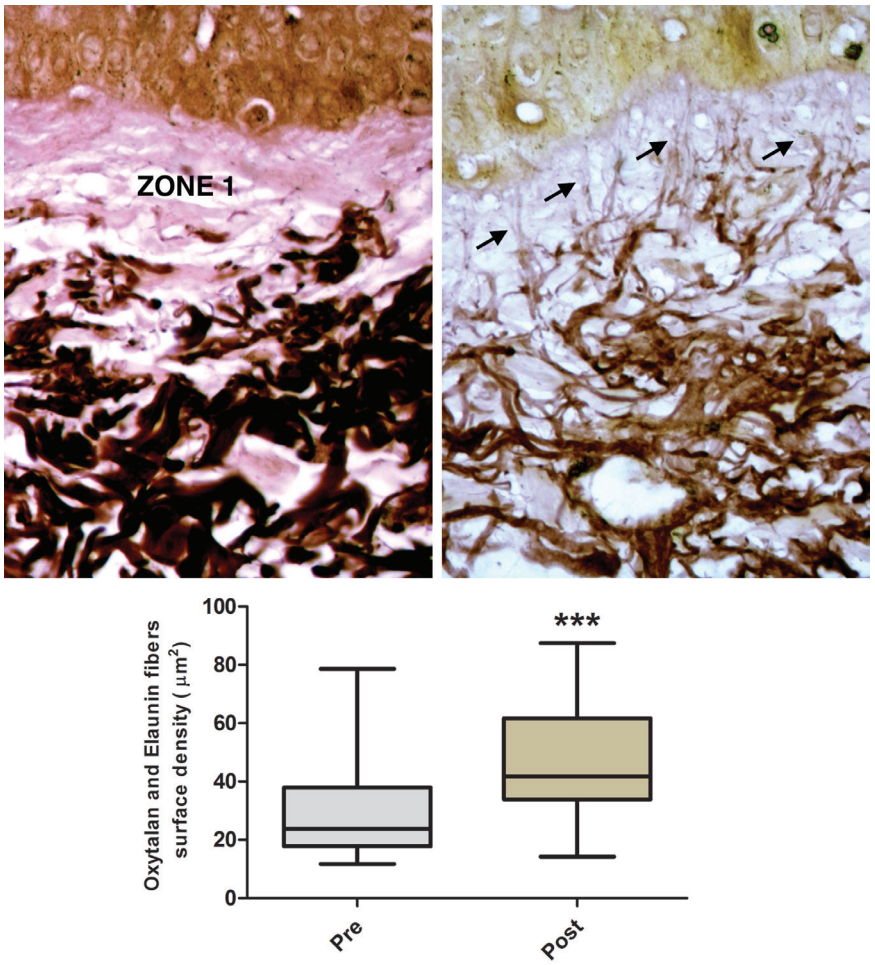

Fig. 1. Elastic fiber system in the dermis zone 1 of treated and nontreated sun-exposed facial skin. (*Above*, *left*) Skin biopsy specimen obtained before adipose-derived stem cell injection: a significant decrease of oxytalan and elaunin fibers in zone 1 of the dermis (median surface density, 23.69 μm²). (*Above*, *right*) Increased and ordered presence of oxytalan and elaunin fibers in zone 1 after adipose-derived stem cell treatment (*arrows*) (median surface density, 41.82 μm²) (orcein staining with previous oxidation; original magnification, × 40); *scale bar* = 25 μm. (*Below*) Graphic representation of the elastic fiber system in zone 1. Differences between both groups were evaluated by means of the Wilcoxon signed rank test ($p = 0.0001$; $n = 20$). A significant increase of the elastic fiber system plexus was achieved with treatment, compared with pretreatment biopsy specimens.

In zone 2, the solar elastosis resulted in accumulation of the dense pathologic elastin (Fig. 2, *above, left*). After the treatment, a major or a full removal of the elastotic material was observed, associated with regeneration of the whole elastic fiber network (Fig. 2, *above, right*), with the structural organization consistent with the normal elasticity of the dermis. A significant decrease of the elastotic material ($p = 0.0014$) was seen in treated skin compared with pretreated dermis (Fig. 2, *below*).

In skin samples of elastotic degeneration in dermis before treatment, both fibrillin and tropoelastin were observed in the deep dermis, but not in zone 1 that underlies the dermal-epidermal junction (Fig. 3, *above, left*, and *third row, left*). Conversely, fibrillin and tropoelastin were observed within zone 1 of the treated skin, their presence being correlated with the formation of new fibers in this zone, in the quality and pattern of polymerization similar to the normal young skin (Figs. 2, *above, right*, and 3, *above right*). The quantitative analysis confirmed a significant increase ($p = 0.0052$) of fibrillin and tropoelastin ($p = 0.0203$) in treated skin (Fig. 3, *second row* and *below*).

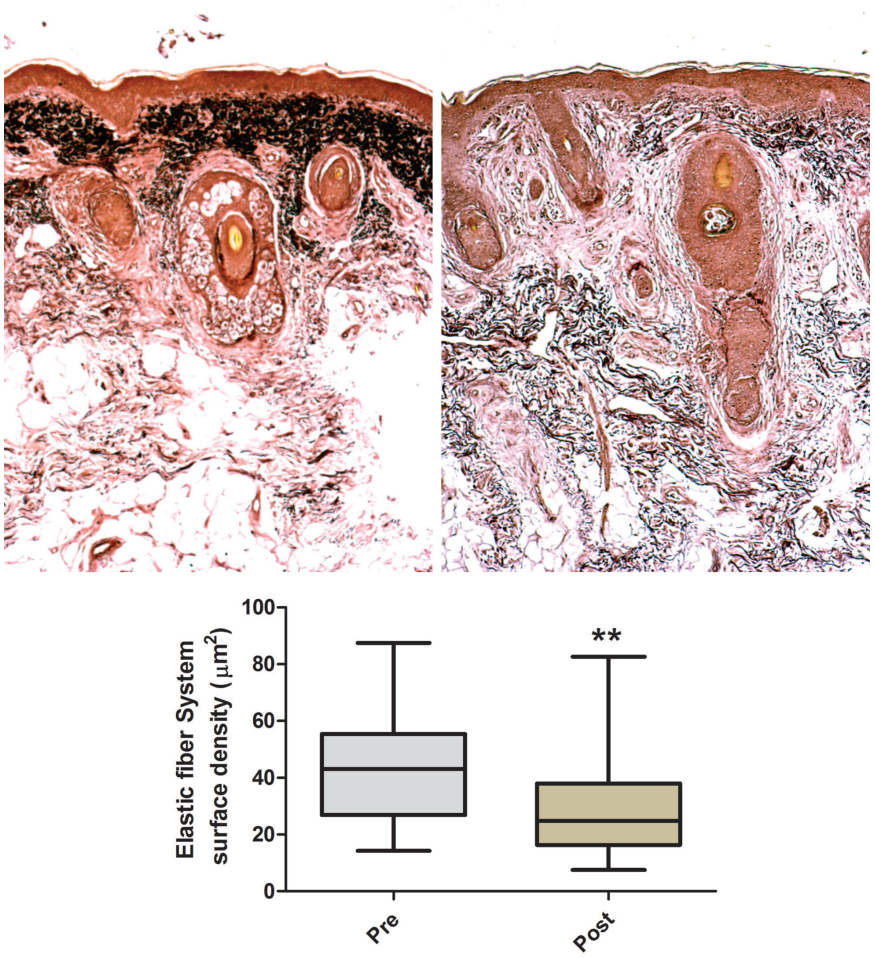

Fig. 2. Elastic fiber system in dermis zone 2 of nontreated and treated sun-exposed facial skin. (*Above, left*) Skin biopsy specimen obtained before adipose-derived stem cell treatment: accumulation of elastotic material (solar elastosis) in zone 2, shown by oxidized orcein staining (median surface density, 43.01 µm²). (*Above, right*) Posttreated skin biopsy specimen showing reduction of the stained elastic mass (elastosis) in reticular dermis (median surface density, 24.75 µm²) (orcein staining with previous oxidation; original magnification, × 10); *scale bar* = 50 µm. (*Below*) Graphic representation of zone 2 elastic system fibers shown by oxidized orcein staining in pretreated and posttreated skin. Differences between both groups were evaluated by means of the Wilcoxon signed rank test ($p = 0.0014$; $n = 20$). A significant decrease of the elastotic material was seen in treated skin compared with pretreated dermis.

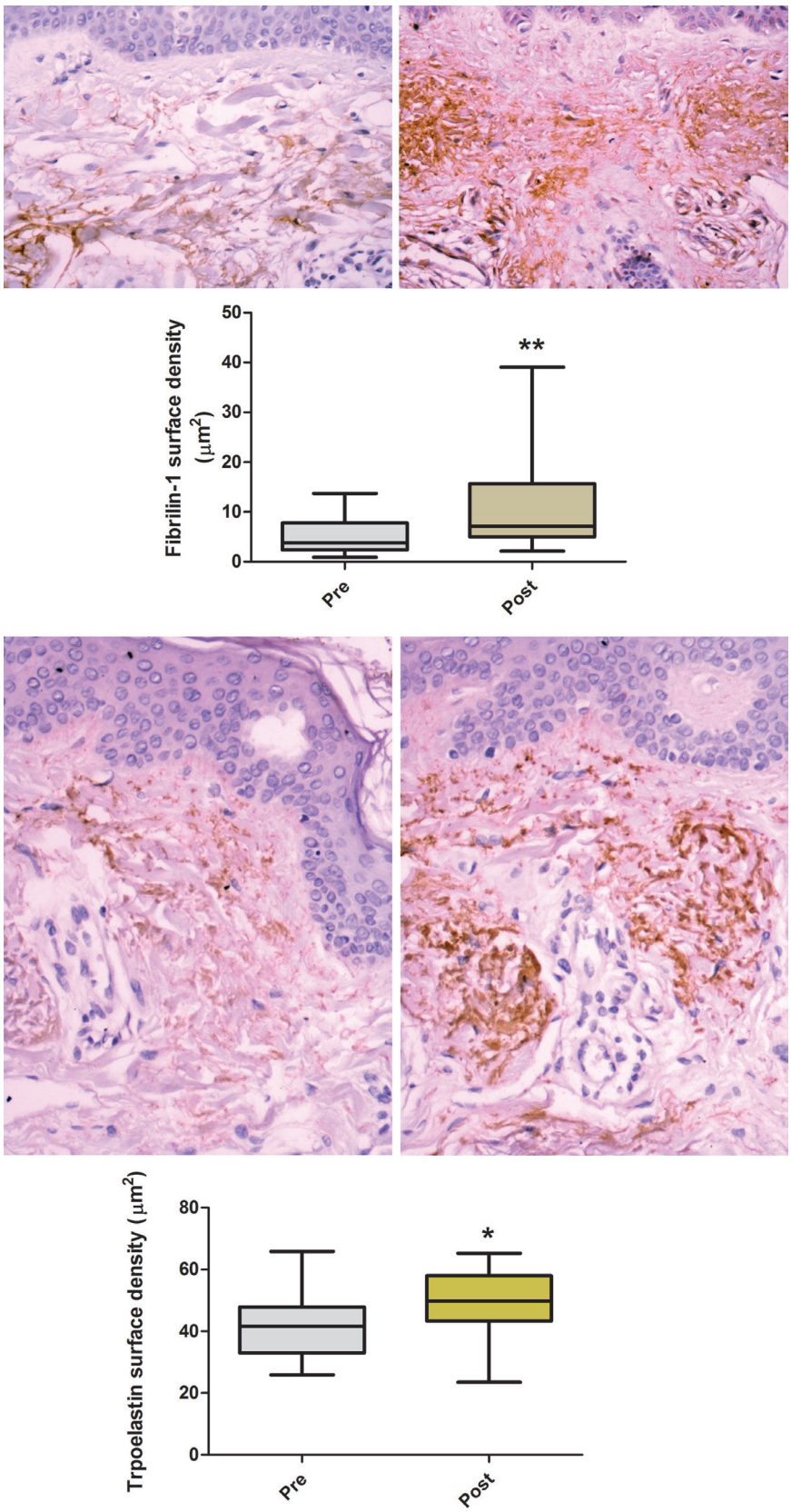

Fig. 3. Fibrillin and tropoelastin immunolabeling in sun-exposed facial skin before and after adipose-derived stem cell injection. (*Above*, *left*) Fibrillin immunolabeling in the pretreated skin biopsy specimen. Absence of fibrillin in zone 1, and its presence in zone 2 as aggregated thick fibers (median surface density, 3.85 μm²) (original magnification, × 40); *scale bar* = 25 μm. (*Above, right*)

In the deep dermis, the total fibrillin and tropoelastin labeling were only slightly increased after treatment, but the morphology of the labeled elastin molecules shifted from amorphous and crumbled elastotic deposits to the normal fibrillary structures (Fig. 3, *above, right*, and *third row, right*). Analysis of the total immunoreactivity of both cathepsin K and matrix metalloproteinase 12 immunolabeling in skin tissues before and after adipose-derived stem cell treatment indicated a significant increase (p = 0.0081 and p = 0.0002, respectively). The activities of the two enzymes were thus potentially complementary (Fig. 4).

We have monitored the markers of the M2 macrophage phenotype in samples of dermal tissue that received the adipose-derived stem cell treatment. Quantification of three markers of the M2 phenotype—CD68, CD206 (mannose receptor), and hemeoxygenase-1—are shown in Figure 5 and **Figure, Supplemental Digital Content 2**. All three showed a significant increase (p = 0.010, p = 0.0107, and $p < 0.0001$, respectively) of positive cells following the adipose-derived stem cell treatment (Fig. 5, *second row* and *below*). [**See Figure, Supplemental Digital Content 2**, which shows hemeoxygenase-1 (*HO-1*) immunostaining in the sun-exposed facial skin before and after adipose-derived stem cell injection. (*Above, left*) Hemeoxygenase-1 immunostaining in pretreated skin biopsy specimen. Rare cells reactive for hemeoxygenase-1 in the dermis of pretreated skin (median surface density, 56.88 μm2). (*Above, right*) Hemeoxygenase-1 levels increased immunoreactivity in the dermis after adipose-derived stem cell treatment (median surface density, 74.70 μm2) (original magnification, × 40); *scale bar* = 25 μm. (*Below*) Graphic representation of hemeoxygenase-1 in inflammatory cells in pretreated and posttreated skin. Differences between both groups were evaluated using the Wilcoxon signed rank test (p = 0.0001; n = 15). Hemeoxygenase-1–reactive cells are significantly increased after adipose-derived stem cell injection, ***http://links.lww.com/PRS/E85***.]

Fig. 3. (*Continued*). Overall increase of fibrillin in the adipose-derived stem cell–treated dermis, including in zone 1 and zone 2 (median surface density, 7.09 μm²). (*Second row*) Graphic representation of fibrillin in dermis of pretreated and treated skin. Differences between both groups were evaluated through Wilcoxon signed rank test (p = 0.0052; n = 14). (*Third row, left*) Tropoelastin immunolabeling in pretreated skin (original magnification, × 40); *scale bar* = 25 μm. Tropoelastin accumulates into zone 2, forming condensed masses of material (median surface density, 41.77 μm²). (*Third row, right*) Reorganization of the tropoelastin reactive material in the posttreatment biopsy specimen. Inset: new tropoelastin in an area of treated skin suggesting elastogenesis. (median surface density, 50 μm²). (*Below*) Graphic representation of the amount of tropoelastin in the skin biopsy specimens. Differences between both groups were evaluated through Wilcoxon signed rank test (p = 0.0203; n = 17). Tropoelastin analysis demonstrated significant increase after adipose tissue–derived mesenchymal stem cell treatment.

DISCUSSION

The present clinical study extends our previous comparative analyses of the facial skin treatments, using enriched fat tissue grafts or adipose-derived stem cells, in which we reported that one of the major modifications in sun-aged skin was regeneration of the dermal elastin.[8] In the present study, inclusion of 20 patients that received adipose-derived stem cell therapy provided new quantitative data, leading to a proposal concerning the involved cellular and molecular mechanisms. We have focused on reduction or full reversal of solar elastosis, addressing two issues: (1) regeneration of the elastic oxytalan and elaunin fibrillary networks lost in the subepidermal papillary dermis, and (2) substitution of pathologic deposits of actinic elastin by a normal elastin fibrillary structure in the deep dermis.

The first question involved a full reactivation of new elastin production and polymerization, within the space in which the normal elastin matrix had been lost during the solar skin-aging. For production of new functional elastin, fibrillin and tropoelastin should be produced and released from cells in a soluble form into the intercellular environment, where they polymerize, giving mature elastic fibers during neoelastinogenesis.[18] In zone 1, selective inhibition of production of these precursor molecules may have occurred, or their input from the underlying dermis was restricted. Both were reversed in the here described adipose-derived stem cell–mediated successful treatment of the sun-aged skin. The high immunoreactivity of the two elastinogenic precursor molecules in regenerating tissues indicated an intense and sufficient de novo formation of normal elastic fiber networks in this zone, which polymerized in a typical complex orthogonal pattern of elastin components in zone 1 (Fig. 1).

Another relevant structural modification of dermis occurred in the same zone following adipose-derived stem cell treatment (Fig. 2). In solar elastosis, a major loss of the papillary

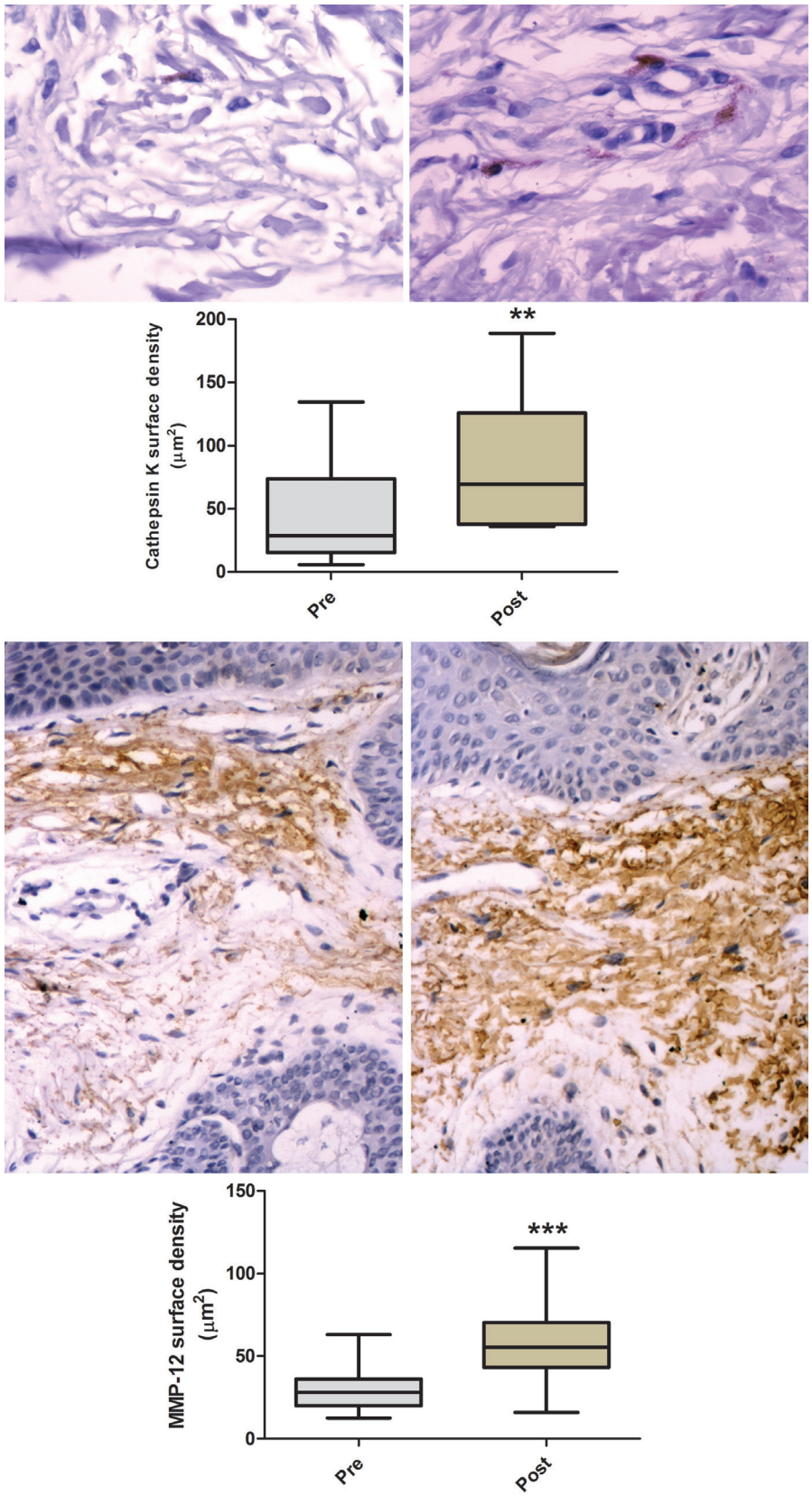

Fig. 4. Cathepsin K and matrix metalloproteinase 12 (*MMP-12*) in sun-exposed facial skin before and after adipose tissue–derived mesenchymal stem cell injection. (*Above*, *left*) Cathepsin K immunostaining in the pretreated skin biopsy specimen. Rare cathepsin K immunoreactive cells in the dermis (median surface density, 28.74 µm²). (*Above, right*) Increase in quantity and reactivity of

organization of the dermal-epidermal junction was always observed, resulting in the flat underlying dermal layer. The papillary design is consistent with an increased flexibility of the overlying epidermal and dermal layers, which can bend together without excessive internal tension. Regeneration of the papillary design may thus also participate in restoring skin elasticity. In contrast, the epidermal proliferative progenitor cells, which continuously renew the epidermal layer, are dependent on their direct cell contact with the basement membrane of the dermal-epidermal junction and on its morphology.[19,20] The flat junction has a lower total interaction surface compared with the papillary one. Its dermal-epidermal basement membrane may be a suboptimal epidermal stem cell niche, and this may be related to the suboptimal epidermal renewal in the elastotic sun-aged skin.

The second question involved ordered the controls of two biochemical regenerative modifications of the deep dermis extracellular matrix: degradation and absorption of excessive elastotic deposits of abnormal elastin, and their substitution by new normally polymerized elastic fiber network in the deep dermis. Mature human elastin is an insoluble and extremely durable protein that normally undergoes very little turnover.[21] However, the pathologic elastotic deposits were efficiently removed during treatment. Cathepsin K can bind to insoluble polymerized elastin in an inactive form, being subsequently remodeled and activated. Cathepsins recognize and have preferences in degrading elastin from different anatomical sites, and they may distinguish the normal elastin from the elastotic deposits in sun-aged skin.[22,23] Total reactivity of cathepsin K increased after mesenchymal stem cell therapy, in terms of both the labeled cell numbers and the label intensity (Fig. 4, *above*).

The normal human skin contains only low levels of cathepsin K. They increase in reparative and hyperplasic processes and after exposition to ultraviolet A both in vivo and in vitro, and these responses decrease in fibroblasts of aged donors.[24,25] The age-related decline of cathepsin K induction could be correlated to the decline of orderly elastin degradation, resulting in accumulation of elastotic skin deposits. Low numbers of cathepsin K–reactive cells observed in the studied patients, increasing after treatment, are consistent with this proposal (Fig. 4).

Cathepsin activity cannot deal with large polymerized elastin fibers, and it depends on previous release of peptides from the extracellular matrix by other enzymes. This requires a group of complementary enzymes involved in the elastinolysis, the metalloproteinases, the major one being potentially the matrix metalloproteinase 12 (macrophage metalloelastase).[26,27] Classic macrophage activation up-regulates several matrix metalloproteinases, but increase of the matrix metalloproteinase 12 mRNA is essentially associated with the alternative macrophage activation in the M2 phenotype.[28] All the mesenchymal stem cells are known to display an antiinflammatory effect in the receptor tissues, in large part because of the induction of monocyte differentiation into M2 macrophages.[29] We understand that differentiation of monocytes incoming from circulation into the treated tissue was directed by the alternative activation toward the M2 tissue macrophages, and this was provided by the introduced adipose-derived stem cells.

Skin repair and regeneration involve cell migration, angiogenesis, tissue environment modifications including controlled inflammation, and extracellular matrix remodeling. In the case of therapeutic use of adipose-derived stem cells, activation of the resident cells can involve all these pathways. The adipose-derived stem cells can produce the required mediators,[14,30] and the long-term activation of the resident mesenchymal stem cell pool by the introduced adipose-derived stem cells can potentially grant extensive and protruded effects of the therapy, such as those observed in our study. However, the resident mesenchymal stem cells were not spontaneously mobilized

Fig. 4. (*Continued*). cathepsin K immunolabeled cells in the dermis of a posttreated skin biopsy specimen (median surface density, 69.50 μm²) (original magnification, × 40); *scale bar* = 25 μm. (*Second row*) Graphic representation of cathepsin K immunolabeling in dermis of pretreated and treated skin. Cathepsin K significantly increased after adipose-derived stem cell injection ($p = 0.0081$; $n = 13$). (*Third row, left*) Matrix metalloproteinase 12 immunostaining in pretreated skin. Matrix metalloproteinase 12 is barely seen in dermis of nontreated skin (median surface density, 28.07 μm²). (*Third row, right*) Matrix metalloproteinase 12 accumulates throughout the dermis after the adipose-derived stem cell treatment (median surface density, 55.48 μm²) (original magnification, × 40); *scale bar* = 25 μm. (*Below*) Graphic representation of percentage of matrix metalloproteinase 12 in the skin biopsy specimens. Differences between both groups were evaluated through the Wilcoxon signed rank test. Matrix metalloproteinase 12 increased significantly after adipose-derived stem cell treatment ($p = 0.0002$; $n = 18$).

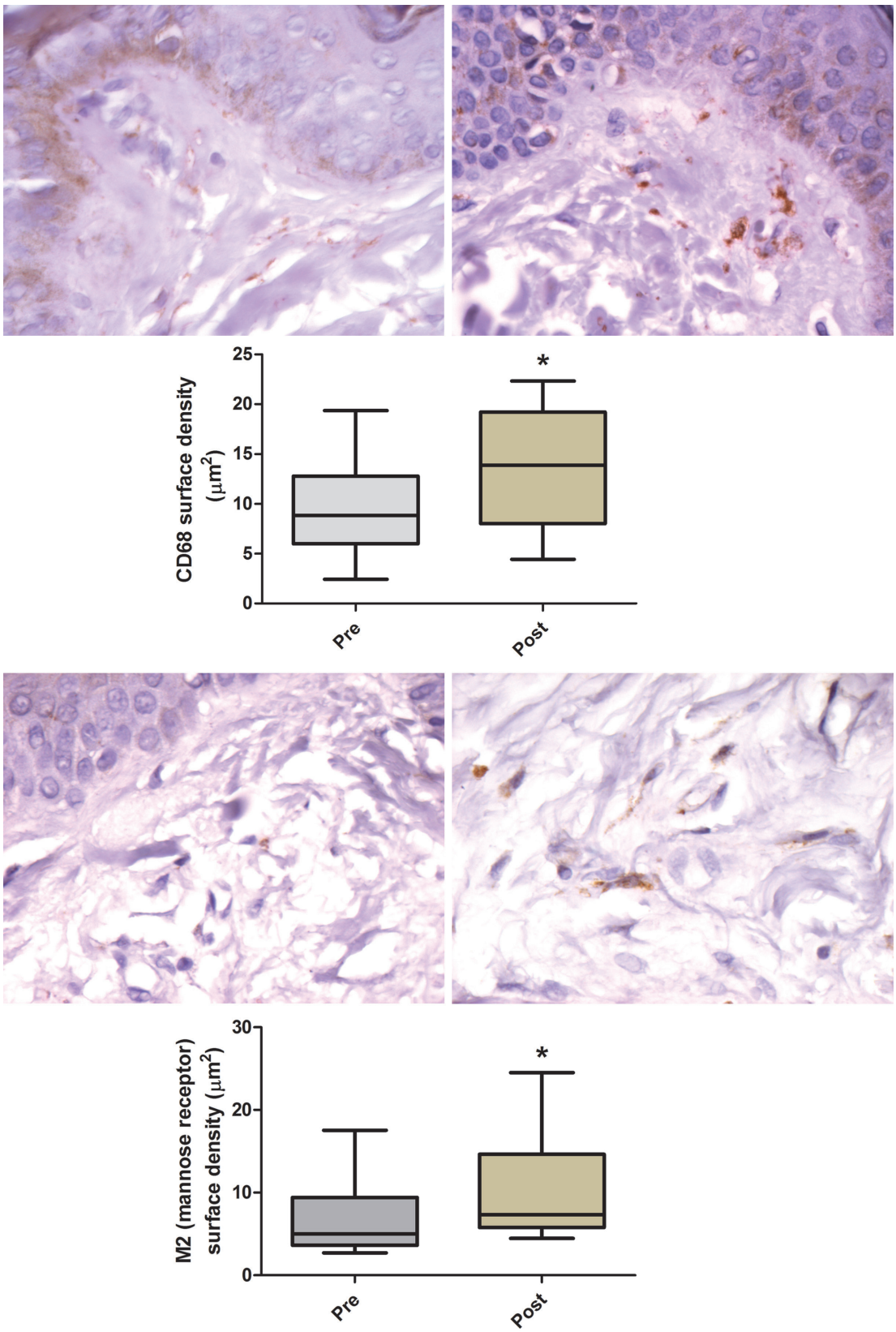

Fig. 5. CD68 and CD206 (mannose receptor) macrophage immunostaining in sun-exposed facial skin before and after adipose-derived stem cell injection. (*Above*, *left*) CD68 immunostaining in the pretreated skin biopsy specimen. Small amount of CD68 macrophages in the dermis of pretreated skin (median surface density, 8.82 μm^2). (*Above, right*) Increase of CD68 reactive macrophages in the

for repair, and previous studies have shown that elastin production declines in aging skin fibroblasts.[31] We have already raised the question of the potentially critical cell quantity required for skin regeneration therapy when following results of lipoaspirate transplant for treatment of radiotherapy lesions.[5] This limitation can be overcome by their in vitro expansion. The present patient series is limited and not sufficient to draw extensive conclusions on the safety of the procedure, but no adverse effects were observed, and our results agree with the worldwide reports on the safety of such therapies.[16] Under strictly controlled conditions of cell manipulation, the adipose-derived stem cell quality can be granted, and the possibility of cryopreservation may open the potential for repeated use, when required.

CONCLUSIONS

Cell-mediated therapies of sun-aged skin lead to full regeneration of dermal elastic matrix components. The present clinical study using subdermal injection of autologous adipose-derived stem cells showed two concomitant and apparently opposed modifications of the elastin matrix: an extensive new production and regeneration of elaunin, oxytalan, and elastin fiber network located in the upper papillary dermis, concomitant with degradation of elastotic abnormal elastin deposits in the deeper dermal layers, which is the major characteristic of solar elastosis. This therapy may be a relevant proposal for the antiaging action in regeneration of the photodamaged human skin.

Fig. 5. (*Continued*). dermis of a posttreated skin biopsy specimen (median surface density, 14 μm²) (original magnification, × 40); *scale bar* = 25 μm. (*Second row*) Graphic representation of CD68⁺ macrophages in pretreated and posttreated skin. Differences between the groups were evaluated through Wilcoxon signed rank test; CD68 macrophages increased significantly after adipose tissue–derived mesenchymal stem cell injection ($p = 0.0105$; $n = 13$). (*Third row, left*) Mannose receptor–reactive cells in pretreated skin. Mannose receptor–reactive macrophages are barely seen in the dermis of nontreated skin (median surface density, 5.01 μm²). (*Third row, right*) After adipose-derived stem cell treatment, mannose receptor–positive macrophages accumulated throughout the dermis (median surface density, 7.34 μm²) (original magnification, × 40); *scale bar* = 25 μm. (*Below*) Graphic representation of the surface density of CD68 and mannose receptor staining in the pretreated and posttreated skin biopsy specimens. Differences between the groups were evaluated using the Wilcoxon signed rank test ($p = 0.0107$; $n = 14$). CD68 and mannose receptor macrophages increased significantly after adipose-derived stem cell treatment.

Luiz Charles-de-Sá, M.D., Ph.D.
Rua Joana Angelica 124/602
22420-030 Rio de Janeiro, Brazil
clinicaperforma@uol.com.br
Instagram: @dr..charlesdesa, @charles_de_sa
Facebook: Charles Sá

ACKNOWLEDGMENT

The authors would like to thank the Coordenação de Aperfeiçoamento de Pessoal de Nível Superior, Brazil, for institutional support.

REFERENCES

1. Strong AL, Neumeister MW, Levi B. Stem cells and tissue engineering: Regeneration of the skin and its contents. *Clin Plast Surg.* 2017;44:635–650.
2. Lee SH, Jin SY, Song JS, Seo KK, Cho KH. Paracrine effects of adipose-derived stem cells on keratinocytes and dermal fibroblasts. *Ann Dermatol.* 2012;24:136–143.
3. Kusuma GD, Carthew J, Lim R, Frith JE. Effect of the microenvironment on mesenchymal stem cell paracrine signaling: Opportunities to engineer the therapeutic effect. *Stem Cells Dev.* 2017;26:617–631.
4. Prockop DJ. Inflammation, fibrosis, and modulation of the process by mesenchymal stem/stromal cells. *Matrix Biol.* 2016;51:7–13.
5. Rigotti G, Marchi A, Galiè M, et al. Clinical treatment of radiotherapy tissue damage by lipoaspirate transplant: A healing process mediated by adipose-derived adult stem cells. *Plast Reconstr Surg.* 2007;119:1409–1422; discussion 1423–1424.
6. Kim JH, Jung M, Kim HS, Kim YM, Choi EH. Adipose-derived stem cells as a new therapeutic modality for ageing skin. *Exp Dermatol.* 2011;20:383–387.
7. Meruane MA, Rojas M, Marcelain K. The use of adipose tissue-derived stem cells within dermal substitutes improves skin regeneration by increasing neoangiogenesis and collagen synthesis. *Plast Reconstr Surg.* 2012;130:53–63.
8. Charles-de-Sá L, Gontijo-de-Amorim NF, Takiya CM, et al. Antiaging treatment of the facial skin by fat graft and adipose-derived stem cells. *Plast Reconstr Surg.* 2015;135:999–1009.
9. Mitchell RE. Chronic solar dermatosis: A light and electron microscopic study of the dermis. *J Invest Dermatol.* 1967;48:203–220.
10. Fisher GJ, Kang S, Varani J, et al. Mechanisms of photoaging and chronological skin aging. *Arch Dermatol.* 2002;138:1462–1470.
11. Fitzpatrick TB. The validity and practicality of sun-reactive skin types I through VI. *Arch Dermatol.* 1988;124:869–871.
12. Zuk PA, Zhu M, Mizuno H, et al. Multilineage cells from human adipose tissue: Implications for cell-based therapies. *Tissue Eng.* 2001;7:211–228.
13. Baptista K, Silva K, Pedrosa C, Borojevic R. Processing of lipoaspirate samples for optimal mesenchymal stem cell isolation. In: Serdev N, ed. *Advanced Techniques in Liposuction and Fat Transfer.* Rijeka, Croatia: Intech; 2011:181–202.
14. Amable PR, Teixeira MV, Carias RB, Granjeiro JM, Borojevic R. Mesenchymal stromal cell proliferation, gene expression and protein production in human platelet-rich plasma-supplemented media. *PLoS One* 2014;9:e104662.
15. Pitanguy I. Face-lifting. In: Pitanguy I, ed. *Aesthetic Plastic Surgery of Head and Body.* New York: Springer-Verlag; 1981:165–200.

16. Lalu MM, McIntyre L, Pugliese C, et al.; Canadian Critical Care Trials Group. Safety of cell therapy with mesenchymal stromal cells (SafeCell): A systematic review and meta-analysis of clinical trials. *PLoS One* 2012;7:e47559.
17. Abbas O, Mahalingam M. The grenz zone. *Am J Dermatopathol.* 2013;35:83–91.
18. Halp[er J, Kjaer M. Basic components of connective tissues and extracellular matrix: Elastin, fibrillin, fibulins, fibrionogen, fibronectin, laminin, tenascins and thrombospondins. *Adv Exp Med Biol.* 2014;802:31–47.
19. Janes SM, Lowell S, Hutter C. Epidermal stem cells. *J Pathol.* 2002;197:479–491.
20. Moon KM, Park YH, Lee JS, et al. The effect of secretory factors of adipose-derived stem cells on human keratinocytes. *Int J Mol Sci.* 2012;13:1239–1257.
21. Schmelzer CE, Jung MC, Wohlrab J, Neubert RH, Heinz A. Does human leukocyte elastase degrade intact skin elastin? *FEBS J.* 2012;279:4191–4200.
22. Novinec M, Grass RN, Stark WJ, Turk V, Baici A, Lenarcic B. Interaction between human cathepsins K, L, and S and elastins: Mechanism of elastinolysis and inhibition by macromolecular inhibitors. *J Biol Chem.* 2007;282:7893–7902.
23. Turk V, Stoka V, Vasiljeva O, et al. Cysteine cathepsins: From structure, function and regulation to new frontiers. *Biochim Biophys Acta* 2012;1824:68–88.
24. Rünger TM, Quintanilla-Dieck MJ, Bhawan J. Role of cathepsin K in the turnover of the dermal extracellular matrix during scar formation. *J Invest Dermatol.* 2007;127:293–297.
25. Codriansky KA, Quintanilla-Dieck MJ, Gan S, Keady M, Bhawan J, Rünger TM. Intracellular degradation of elastin by cathepsin K in skin fibroblasts: A possible role in photoaging. *Photochem Photobiol.* 2009;85:1356–1363.
26. Saarialho-Kere U, Kerkelä E, Jeskanen L, et al. Accumulation of matrilysin (MMP-7) and macrophage metalloelastase (MMP-12) in actinic damage. *J Invest Dermatol.* 1999;113:664–672.
27. Taddese S, Weiss AS, Neubert RH, Schmelzer CE. Mapping of macrophage elastase cleavage sites in insoluble human skin elastin. *Matrix Biol.* 2008;27:420–428.
28. Huang WC, Sala-Newby GB, Susana A, Johnson JL, Newby AC. Classical macrophage activation up-regulates several matrix metalloproteinases through mitogen activated protein kinases and nuclear factor-κB. *PLoS One* 2012;7:e42507.
29. Zachar L, Bačenková D, Rosocha J. Activation, homing, and role of the mesenchymal stem cells in the inflammatory environment. *J Inflamm Res.* 2016;9:231–240.
30. Kim BS, Gaul C, Paul NE, et al. The effect of lipoaspirates on human keratinocytes. *Aesthet Surg J.* 2016;36:941–951.
31. Sephel GC, Davidson JM. Elastin production in human skin fibroblast cultures and its decline with age. *J Invest Dermatol.* 1986;86:279–285.